


## Enhancing Synchronization by Optimal Correlated Noise

Sherwood Martineau<sup>1</sup>, Tim Saffold, Timothy T. Chang<sup>1</sup>, and Henrik Ronellenfitsch<sup>1\*</sup>  
*Physics Department, Williams College, 33 Lab Campus Drive, Williamstown, Massachusetts 01267, USA*

 (Received 13 July 2021; revised 11 January 2022; accepted 9 February 2022; published 1 March 2022)

From the flashes of fireflies to Josephson junctions and power infrastructure, networks of coupled phase oscillators provide a powerful framework to describe synchronization phenomena in many natural and engineered systems. Most real-world networks are under the influence of noisy, random inputs, potentially inhibiting synchronization. While noise is unavoidable, here we show that there exist optimal noise patterns which minimize desynchronizing effects and even enhance order. Specifically, using analytical arguments we show that in the case of a two-oscillator model, there exists a sharp transition from a regime where the optimal synchrony-enhancing noise is perfectly anticorrelated, to one where the optimal noise is correlated. More generally, we then use numerical optimization methods to demonstrate that there exist anticorrelated noise patterns that optimally enhance synchronization in large complex oscillator networks. Our results may have implications in networks such as power grids and neuronal networks, which are subject to significant amounts of correlated input noise.

DOI: [10.1103/PhysRevLett.128.098301](https://doi.org/10.1103/PhysRevLett.128.098301)

The occurrence of noise is unavoidable in networks and systems at all scales [1], from biological examples [2] such as neurons in the auditory and visual pathways [3–5] and neural information processing [6,7] to mechanical oscillators [8] and fluctuating inputs affecting the stability of power grids [9–11]. Synchronization of the underlying network of nonlinear phase oscillators is a paradigm employed to understand such physical and biological networks [12,13]. Fluctuations are generally seen as undesirable, and significant efforts have been made to understand and prevent their detrimental effects on network synchronization [14–19]. Optimization methods have been successfully employed to improve synchrony with and without noise, in particular by adjusting the weighted network topology [17,20–28]. Similar techniques have also been effective for other types of networks and objectives such as efficient transport [29–35]. There has been recent interest in the possibility that noise may be leveraged to enhance synchronization [36–43]. Specifically, it was found that the degree to which input noise is correlated may have a significant influence on its ability to aid in or prevent network synchrony [36].

Based on the widely used Kuramoto model [44,45], here we study the optimal patterns of input noise correlations that enhance synchronization in networks of oscillators. Using analytic arguments we find that in the simple case of two coupled oscillators in the phase-drift regime as studied in Ref. [36], the optimal synchrony-enhancing noise undergoes a transition from perfect anticorrelation to perfect correlation as the total noise strength is increased. We then numerically study generic complex networks near phase-locked fixed points and show that the optimal pattern of synchrony-enhancing noise retains essential characteristics

seen in the two-oscillator case. The optimal noise we uncover is strongly linked to the network topology. In complex networks, the optimal noise correlations show characteristic clustering, separating the network into regions that benefit from receiving uncorrelated inputs. We now proceed to analytically study the tractable case of two connected Kuramoto oscillators subject to generic noise.

The model consists of coupled phase oscillators with different natural frequencies. In the limit of weak coupling, the phases can be modeled using the Kuramoto-type equations

$$\begin{aligned}\frac{d\theta_1}{dt} &= \omega_1 + \frac{K}{2} \sin(\theta_2 - \theta_1) + \eta_1 \\ \frac{d\theta_2}{dt} &= \omega_2 + \frac{K}{2} \sin(\theta_1 - \theta_2) + \eta_2,\end{aligned}\quad (1)$$

where  $\theta_i(t)$  are the oscillator phases,  $\omega_i$  the natural frequencies,  $K$  is the coupling constant, and  $\eta_i$  are stochastic white noise terms satisfying  $\langle \eta_i \rangle = 0$  and  $\langle \eta_i(t) \eta_j(t') \rangle = C_{ij} \delta(t - t')$  with the symmetric and positive semidefinite covariance matrix  $C_{ij} = C_{ji}$ . The model described by Eq. (1) was recently shown to exhibit counterintuitive enhanced synchronization under uncorrelated noise  $C_{ij} \sim \delta_{ij}$  as opposed to common noise  $C_{ij} = C$  [36]. We now study this effect allowing for arbitrary correlations between the noise terms. It is useful to change variables to the mean angle  $\mu = (\theta_1 + \theta_2)/2$  and angular difference  $\delta = \theta_1 - \theta_2$ . The mean  $\mu$  is irrelevant for synchronization as quantified by the squared Kuramoto order parameter  $R^2 = |\sum_j e^{i\theta_j}/N|^2 = 1/2 + (1/2) \cos \delta$ . We focus on the equation for the phase difference,

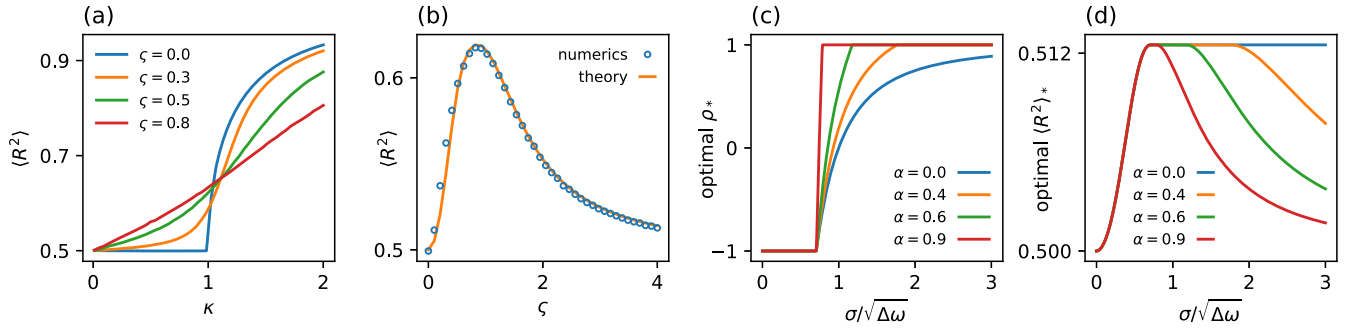


FIG. 1. Noise-enhanced synchronization in the two-oscillator model and optimal covariance transition. (a) Numerically obtained  $\langle R^2 \rangle$  from integrating Eq. (2) until  $\tau = 400\,000$  from random initial conditions as a function of  $\kappa = K/\Delta\omega$  for several  $\zeta$ . (b) Numerically obtained  $\langle R^2 \rangle$  from integrating Eq. (2) until  $\tau = 20\,000$  from random initial conditions (circles) and analytic approximation (see the Supplemental Material [47], Sec. I for the explicit formula) as a function of  $\zeta$  for  $\kappa = 0.9$ . (c) Numerically approximated optimal covariance  $\rho_*$ . To simplify comparing between different combinations of  $\sigma_{1,2}$ , we introduced the average  $\sigma = (\sigma_1 + \sigma_2)/2$  and the relative difference  $\alpha = |\sigma_1 - \sigma_2|/(\sigma_1 + \sigma_2)$ . Optimal correlations were obtained at  $\kappa = 0.1$ . The transitions occur at  $\sigma_a/\sqrt{\Delta\omega} \approx 1/\sqrt{2}$  and  $\sigma_c/\sqrt{\Delta\omega} \approx 1/(\alpha\sqrt{2})$ . (d) Approximate optimal order parameter  $\langle R^2 \rangle_*$  for the optimal covariances shown in panel (c) at  $\kappa = 0.1$ .

$$\delta'(\tau) = 1 - \kappa \sin \delta(\tau) + \zeta, \quad (2)$$

where the prime indicates a derivative with respect to  $\tau = \Delta\omega t$ , the dimensionless parameter  $\kappa = K/\Delta\omega$ , and the dimensionless noise  $\zeta = (\eta_1 - \eta_2)/\Delta\omega$ .

In the absence of noise,  $\zeta = 0$ , it is well known that Eq. (2) exhibits a synchronization transition at  $\kappa = 1$  [44,46]. To study nonvanishing noise, we calculate  $\langle \zeta \rangle = 0$  and

$$\begin{aligned} \langle \zeta(\tau)\zeta(\tau') \rangle &= \frac{1}{\Delta\omega} (C_{11} - 2C_{12} + C_{22})\delta(\tau - \tau') \\ &= 2\zeta^2\delta(\tau - \tau'). \end{aligned}$$

This suggests that  $\zeta^2 = (C_{11} - 2C_{12} + C_{22})/(2\Delta\omega)$  is the relevant effective noise strength for synchronization. This effective noise strength depends on the correlation between the original noise inputs  $\eta_{1,2}$ . Specifically, for common noise,  $C_{ij} = \sigma^2$  implies  $\zeta^2 = 0$ : Common noise does not affect synchronization at all. For uncorrelated noise,  $C_{ii} = \sigma^2$  and  $C_{12} = 0$ , which implies  $\zeta^2 = \sigma^2/\Delta\omega$ . A similar argument shows that the maximum effective noise strength for synchronization is achieved for *anti-correlated* inputs  $C_{ii} = \sigma^2$ ,  $C_{12} = -\sigma^2$  with  $\zeta^2 = 2\sigma^2/\Delta\omega$ .

But how does  $\zeta^2$  affect synchronization, and can we find an optimal noise correlation? We numerically simulated Eq. (2) and computed long-time averages of the order parameter  $\langle R^2 \rangle$  for several  $\zeta^2$ . In the regime below the transition,  $\kappa < 1$ , noise generally enhances synchronization, while for  $\kappa > 1$ , noise generally decreases synchronization [Fig. 1(a), Ref. [36]]. At fixed  $\kappa$ , there exists an optimal effective noise  $\zeta_*^2$  that maximizes synchronization [Fig. 1(b)].

We can relate this to the original noise covariance matrix as follows. Fixing the noise variances  $C_{ii} = \sigma_i^2$ , the covariance  $C_{12} = \sigma_1\sigma_2\rho$  with the correlation

$-1 \leq \rho \leq 1$  can be used to tune the effective noise and thus increase synchronization. While it appears straightforward to obtain the optimal  $\zeta_*^2$  and then to solve  $\zeta_*^2 = (\sigma_1^2 - 2\sigma_1\sigma_2\rho + \sigma_2^2)/(2\Delta\omega)$  for the correlation  $\rho$ , the constraint  $-1 \leq \rho \leq 1$  must be taken into account: it is not always possible to adjust  $\rho$  and reach the optimal  $\zeta_*^2$ . When this happens, the optimal correlation occurs at the boundary of the allowed range,  $\rho_* = \pm 1$ . Solving for  $\rho_*$ , the optimal correlation to enhance synchronization at fixed  $\sigma_{1,2}$  is then

$$\rho_* = \left[ \frac{\sigma_1^2 + \sigma_2^2}{2\sigma_1\sigma_2} - \frac{\zeta_*^2\Delta\omega}{\sigma_1\sigma_2} \right]', \quad (3)$$

where the primed angle brackets indicate that the argument is clipped to remain between  $-1$  and  $1$  using  $[x]' = \min[\max(x, -1), 1]$ . This clipping leads to a sharp transition [Figs. 1(c) and 1(d)]. In the following, it is useful to introduce the average  $\sigma = (\sigma_1 + \sigma_2)/2$ . For small  $\sigma/\sqrt{\Delta\omega}$ , anticorrelated noise optimally enhances synchronization [Fig. 1(c)]. Solving Eq. (3) for  $\rho_* = -1$ , we find the critical noise strength  $\sigma_a$  below which anticorrelated noise is optimal,  $\sigma_a = \zeta_*\sqrt{\Delta\omega}/2$ . Similarly, solving Eq. (3) for  $\rho_* = +1$ , we find the critical noise strength  $\sigma_c$  above which common noise is optimal,  $\sigma_c = \sigma_a/\alpha$ , where  $\alpha = |\sigma_1 - \sigma_2|/(\sigma_1 + \sigma_2)$ . In the regime where  $-1 < \rho_* < 1$ , the global optimum can be reached, and  $\langle R^2 \rangle_*$  is constant. Otherwise, the optimal order parameter occurs at the boundary of the allowed range of  $\rho$  and is less than the global maximum. In this case,  $\rho_* = \pm 1$  [Fig. 1(c)].

While  $\zeta_*^2$  and thus  $\rho_*$  can be obtained numerically, it is possible to gain insight from an analytic approximation. Equation (2) is equivalent to the Fokker-Planck equation

$$\frac{\partial p(\delta, t)}{\partial t} = -\frac{\partial}{\partial \delta} [(1 - \kappa \sin \delta) p(\delta, t)] + \zeta^2 \frac{\partial^2 p(\delta, t)}{\partial \delta^2} \quad (4)$$

for the probability density  $p(\delta + 2\pi, t) = p(\delta, t)$ . From a Fourier series approximation to the solution of Eq. (4), we obtain an explicit expression for  $\langle R^2 \rangle(\zeta, \kappa)$  in the regime of small  $\kappa$  [47]. The optimal effective noise is then  $\zeta_*^2 = 1 - (23/100)\kappa^2 + \mathcal{O}(\kappa^4)$ , and the corresponding maximal order parameter is  $\langle R^2 \rangle_* = 1/2 + (\kappa/8) + \mathcal{O}(\kappa^3)$ . Even for larger  $\kappa \lesssim 1$ , there is good agreement with full numerical solutions of the Fokker-Planck equation [Fig. 1(b), Supplemental Material [47], Sec. I]. The situation is different in the regime  $\kappa > 1$  where phase-locked fixed points exist. Here, common noise is always optimal, and the noise-free order parameter  $R_0^2$  can not be exceeded (Supplemental Material [47], Sec. II).

In many real-world cases such as power grids, the network operates near a phase-locked fixed point instead of in the incoherent regime. Therefore, we now focus on general networks near a fixed point and show that, unlike in the two-oscillator case, there exist optimal correlation patterns beyond common noise that enhance synchronization. While we note that other order parameters can also be relevant [53], here we consider the Kuramoto order parameter. The equations of motion for  $N$  coupled oscillators are

$$\frac{d\theta_i}{dt} = \omega_i + \sum_{j=1}^N K_{ij} \sin(\theta_j - \theta_i) + \eta_i, \quad (5)$$

where again the stochastic forcing is given by correlated white noise,  $\langle \eta_i(t) \eta_j(t') \rangle = C_{ij} \delta(t - t')$  and  $\langle \eta_i \rangle = 0$ . The matrix  $K_{ij} = K_{ji}$  encodes the weighted network topology. Equation (5) as well as the order parameter allow one to shift the phases as  $\theta_i \rightarrow \theta_i - \mu$ , where  $\mu$  is the mean phase. In the following, we adopt these ‘‘centered dynamics,’’ where the mean natural frequency, the mean noise, and the mean covariance with any oscillator vanish,  $\sum_i \omega_i = \sum_j \eta_j = \sum_j C_{ij} = 0$  (Supplemental Material [47], Sec. III). Note that noise that is uncorrelated in the original frame ( $C_{ij} \sim \delta_{ij}$ ) appears uniformly correlated in centered dynamics,  $C_{ij} \sim \delta_{ij} + (\delta_{ij} - 1)/(N - 1)$ . Assuming that weak noise drives the centered Eq. (5) near a fixed point  $0 = \omega_i + \sum_{j=1}^N K_{ij} \sin(\bar{\theta}_j - \bar{\theta}_i)$ , we expand  $\theta_i = \bar{\theta}_i + \varepsilon_i$  to obtain the linearized dynamics of the perturbations  $\varepsilon_i$ ,

$$\frac{d\varepsilon_i}{dt} = \sum_{j=1}^N K_{ij} \cos(\bar{\theta}_j - \bar{\theta}_i) (\varepsilon_j - \varepsilon_i) + \eta_i. \quad (6)$$

In the following, we are interested in long-time averages such that any initial transients have decayed and the system has settled into an equilibrium distribution. We expand the order parameter averaged in this way,

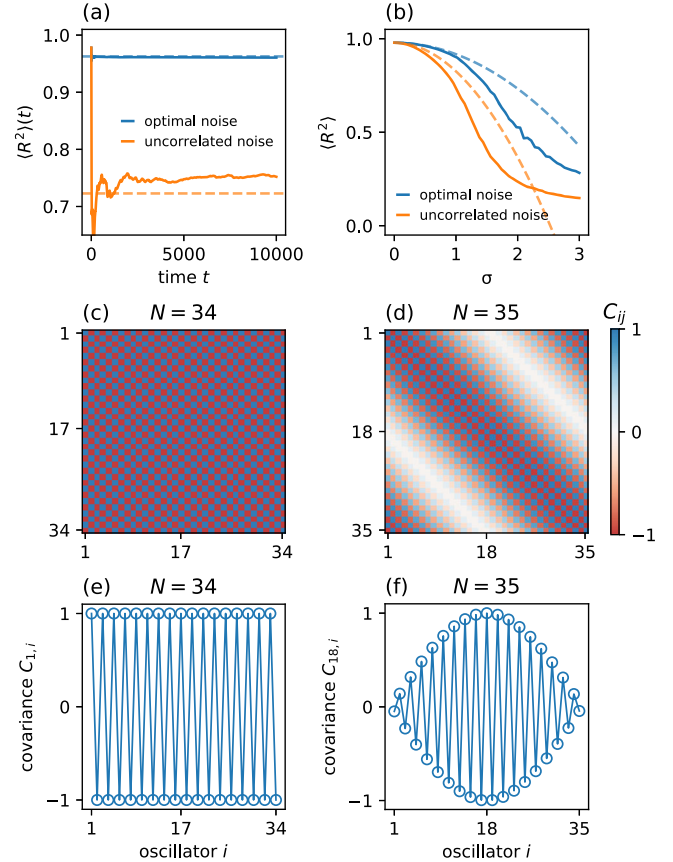


FIG. 2. Optimal noise patterns in periodic oscillator chains near fixed points. (a) Time-averaged order parameter  $\langle R^2 \rangle(t) = (1/t) \int_0^t R^2(t') dt'$  in a periodic chain of  $N = 54$  oscillators for optimal and uncorrelated noise. Dashed lines correspond to model predictions from Eq. (7). The noise variance  $\sigma = 0.5$ . (b) Numerically obtained long-time order parameters  $\langle R^2 \rangle$  in an  $N = 20$  periodic chain of oscillators with optimal and uncorrelated noise. Dashed lines correspond to model predictions; order parameters were obtained at  $t = 15\,000$ . (c) Optimal covariance matrix for even periodic chain of  $N = 34$ . (d) Optimal covariance matrix for odd periodic chain of  $N = 35$ . (e) Optimal covariances  $C_{1,i}$  with respect to the first oscillator in the even chain. (f) Frustrated optimal covariance pattern  $C_{18,i}$  with respect to the center oscillator in the odd chain. Natural frequencies in all panels were drawn from the normal distribution  $\mathcal{N}(0, 1/N^2)$ , and  $K = 2$ .

$$\langle R^2 \rangle = R_0^2 + \frac{1}{2} \langle \mathbf{e}^\top H \mathbf{e} \rangle + \mathcal{O}(\varepsilon^3), \quad (7)$$

where  $R_0^2$  is the order parameter at the fixed point  $\bar{\theta}_i$ , and the angle brackets denote the long-time average. The linear term  $\langle J \mathbf{e} \rangle = J \langle \mathbf{e} \rangle$ , where  $J$  is the Jacobian matrix, vanishes due to  $\langle \mathbf{e} \rangle = 0$ . The Hessian matrix  $H_{ij} = (2/N^2) [\cos(\bar{\theta}_i - \bar{\theta}_j) - \delta_{ij} \sum_k \cos(\bar{\theta}_i - \bar{\theta}_k)]$  encodes the synchronization state of the fixed point and is negative semidefinite close to the synchronous state  $\bar{\theta}_i \approx 0$  (Supplemental Material [47], Sec. VI), but can be positive semidefinite or even indefinite, for instance

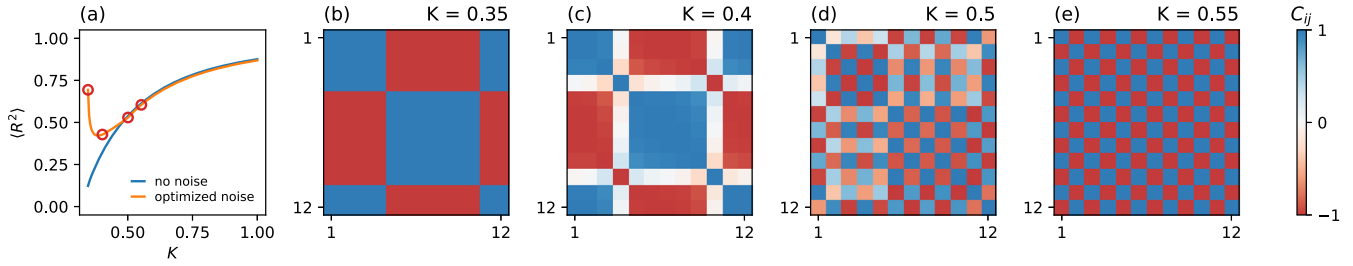


FIG. 3. Optimal noise covariance matrix near the synchronization transition in a  $N = 12$  ring of oscillators. (a) Optimal noise significantly enhances the approximate order parameter  $\langle R^2 \rangle = R_0^2 + (1/2)\sigma^2 \text{tr}(HE)$  close to the synchronization transition. Shown are curves with  $\sigma = 0.25$  and  $\sigma = 0$  (no noise). (b)–(e) Optimal covariance matrices near the synchronization transition. The locations corresponding to the matrices in panels (b)–(e) are marked (red circles) in panel (a). Close to the phase-drift regime (small  $K$ ), the optimal covariances are large-scale ordered and then transition to local order.

close to “twisted states” (Ref. [48] and Supplemental Material [47], Sec. VI). Thus, we expect that noise will generically reduce synchrony. However, it is still possible to find noise inputs that minimize these effects, and transitions can occur. Equation (7) suggests that such optimal synchronization is achieved by maximizing the second-order term  $\langle \mathbf{e}^\top H \mathbf{e} \rangle = \text{tr}(HE)$ . Here,  $\text{tr}(\cdot)$  is the matrix trace, and  $E = \langle \mathbf{e} \mathbf{e}^\top \rangle$  satisfies the continuous Lyapunov equation  $LE + EL = -C$  for the weighted Laplacian matrix  $L_{ij} = K_{ij} \cos(\bar{\theta}_j - \bar{\theta}_i) - \delta_{ij} \sum_n K_{in} \cos(\bar{\theta}_n - \bar{\theta}_i)$ . This can be seen by formally solving Eq. (6) in the Langevin formalism and performing the noise average (Supplemental Material [47], Sec. V). The Lyapunov equation frequently occurs in stability and control theory [49]. Our goal of finding the optimal noise covariances  $C$  can be formulated as the constrained optimization problem

$$\begin{aligned} & \max_{C, E} \quad \text{tr}(HE) \\ & \text{such that} \quad LE + EL = -C \\ & \quad \quad \quad C \succeq 0. \end{aligned} \quad (8)$$

A valid covariance matrix must be positive semidefinite,  $C \succeq 0$ . This constraint turns the problem into a semidefinite program [54]. As it stands, the optimization problem is unbounded, such that we must augment it by an additional constraint to set the noise scale. For simplicity, we fix uniform variances,  $C_{ii} = 1$ . Because the Lyapunov equation in Eq. (8) is linear, any uniform  $C_{ii}$  can be obtained by rescaling the optimal solution. Because of the centered frame constraint  $\sum_j C_{ij} = 0$  we expect anticorrelations to be relevant in complex networks again.

To uncover the relationship between network topology and optimal noise, we numerically analyze networks of increasing complexity. For simplicity, we take the coupling constants to be uniform,  $K_{ij} \equiv K/d$ , where  $d$  is the network’s average degree. We draw the natural frequencies from a Gaussian distribution  $\omega_i \sim \mathcal{N}(0, 1/N^2)$ , where  $N$  is the number of nodes. The mean of the natural frequencies for each network is set to exactly zero. Fixed points and

solutions to the semidefinite program in Eq. (8) are obtained numerically (Supplemental Material [47], Sec. IV).

As the simplest extension of our two-oscillator model we first consider periodic chains of  $N$  oscillators. We note that the optimal noise pattern obtained from solving Eq. (8) is highly effective in improving synchronization as compared with uncorrelated noise [Fig. 2(a)], even far into the nonlinear regime [Fig. 2(b)]. Interestingly, the optimal noise is such that neighboring pairs in chains with an even number of oscillators receive anticorrelated inputs [Figs. 2(c) and 2(e)]. However, it is not always possible for all pairs of neighbors in a network to receive perfectly anticorrelated inputs, leading to frustrated patterns of optimal noise. Indeed, for an odd number of oscillators in the chain, the magnitude of the optimal noise correlation  $|C_{ij}|$  decays away from any particular oscillator  $i$ . The chain topology prevents any two neighboring oscillators from receiving perfectly anticorrelated noise [Figs. 2(d) and 2(f)]. This effect is also seen in periodic grids (Supplemental Material [47], Sec. VIII). It is interesting to note that the optimal noise itself may exhibit a transition from local to global organization near the synchronization transition of the underlying network, depending on the specific set of natural frequencies  $\omega_i$  [Fig. 3]. The transition is accompanied by a significant increase of the order parameter [Fig. 3(a)] that even persists into the phase-drift regime for a large region of couplings  $K$  (Supplemental Material [47], Sec. IX).

We finally consider complex network topologies derived from power grids [55]. Here, the optimal noise patterns show clustering, where groups of oscillators are approximately anticorrelated among themselves. Correlations between the clusters are approximately zero (Fig. 4), potentially promoting cluster synchronization [56]. One particular type of cluster in these networks consists of one single “dangling” node together with its neighbor. Such nodes have been identified as vulnerable to perturbations before [57,58]. Real power grid dynamics can be modeled using a second-order model [9] which is also amenable to our method and shows a dependence of the optimal



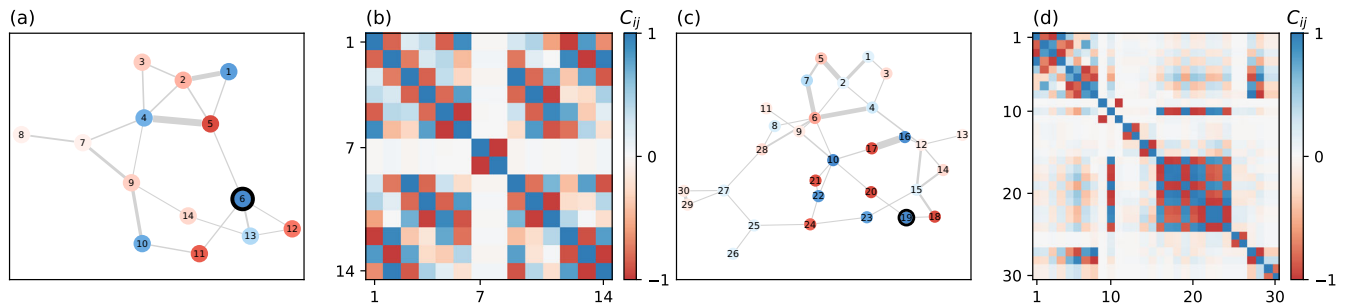


FIG. 4. Anti-correlated patterns form clusters in complex networks. (a) IEEE 14-node test grid, node colors corresponds to correlation with oscillator 6. (b) Optimal covariance matrix for the network from (a). There are two clusters of anti-correlated oscillators that are uncorrelated with each other. (c) IEEE 30-node test grid, node colors corresponds to correlation with oscillator 19. (d) Optimal covariance matrix for the network from (c). There are several clusters of anti-correlated oscillators that are uncorrelated with each other. Small clusters of two nodes generally have one of the nodes “dangling” with only one neighbor. In all graph plots, edge width is proportional to the coupling strength  $K_{ij}$ . Power loads were centered and normalized to unit variance, and then used as constant inputs.

covariances on the inertia in the network (Supplemental Material [47], Sec. X).

We studied to what extent synchronization in complex oscillator networks can be enhanced by correlated noise. We showed that in the phase-drift regime of a two-oscillator system, optimal noise correlations can significantly improve synchronization. The optimal correlations exhibit a transition between anticorrelated and correlated noise depending on the overall noise strength. In complex networks, we found that the optimal input noise is generally anticorrelated with diverse patterns where the strength of correlations can be constant, decaying, or even be restricted to clusters of oscillators.

Our results may have implications for real networks such as power grids and neuronal networks. For instance, power grid synchronization may be enhanced if new power plants and lines are judiciously placed according to the principles outlined above. Correlations of input noise can be estimated [59], or predicted from the weather [60,61]. Our work opens up new pathways to understanding and controlling synchronization in complex systems.

S. M., T. S., and T. T. C. acknowledge support from the Williams College Science Center.

\*henrik.ronellenfitch@gmail.com

- [1] B. Lindner, Effects of noise in excitable systems, *Phys. Rep.* **392**, 321 (2004).
- [2] D. K. Wells, W. L. Kath, and A. E. Motter, Control of Stochastic and Induced Switching in Biophysical Networks, *Phys. Rev. X* **5**, 031036 (2015).
- [3] W. Bialek, Physical limits to sensation and perception, *Annu. Rev. Biophys. Biophys. Chem.* **16**, 455 (1987).
- [4] L. S. Tsimring, Noise in biology, *Rep. Prog. Phys.* **77**, 026601 (2014).
- [5] J. Shlens, F. Rieke, and E. Chichilnisky, Synchronized firing in the retina, *Curr. Opin. Neurobiol.* **18**, 396 (2008).
- [6] H. G. Eyherabide and I. Samengo, When and why noise correlations are important in neural decoding, *J. Neurosci.* **33**, 17921 (2013).
- [7] I. Kanitscheider, R. Coen-Cagli, and A. Pouget, Origin of information-limiting noise correlations, *Proc. Natl. Acad. Sci. U.S.A.* **112**, E6973 (2015).
- [8] M. H. Matheny, J. Emenheiser, W. Fon, A. Chapman, A. Salova, M. Rohden, J. Li, M. Hudoba de Bady, M. Pósfai, L. Duenas-Osorio, M. Mesbahi, J. P. Crutchfield, M. C. Cross, R. M. D’Souza, and M. L. Roukes, Exotic states in a simple network of nanoelectromechanical oscillators, *Science* **363**, eaav7932 (2019).
- [9] P. H. Nardelli, N. Rubido, C. Wang, M. S. Baptista, C. Pomalaza-Raez, P. Cardieri, and M. Latva-aho, Models for the modern power grid, *Eur. Phys. J. Special Topics* **223**, 2423 (2014).
- [10] P. Milan, M. Wächter, and J. Peinke, Turbulent Character of Wind Energy, *Phys. Rev. Lett.* **110**, 138701 (2013).
- [11] B. Schäfer, C. Beck, K. Aihara, D. Witthaut, and M. Timme, Non-Gaussian power grid frequency fluctuations characterized by Lévy-stable laws and superstatistics, *Nat. Energy* **3**, 119 (2018).
- [12] S. Strogatz, *Sync: How Order Emerges from Chaos In the Universe, Nature, and Daily Life* (Hachette Books, New York, 2012).
- [13] R. E. Mirollo and S. H. Strogatz, Synchronization of pulse-coupled biological oscillators, *SIAM J. Appl. Math.* **50**, 1645 (1990).
- [14] C. Luo and H. Banakar, Strategies to smooth wind power fluctuations of wind turbine generator, *IEEE Trans. Energy Convers.* **22**, 341 (2007).
- [15] B. C. Bag, K. G. Petrosyan, and C.-K. Hu, Influence of noise on the synchronization of the stochastic Kuramoto model, *Phys. Rev. E* **76**, 056210 (2007).
- [16] T. Yanagita and A. S. Mikhailov, Design of oscillator networks with enhanced synchronization tolerance against noise, *Phys. Rev. E* **85**, 056206 (2012).

- [17] H. Ronellenfitch, J. Dunkel, and M. Wilczek, Optimal Noise-Canceling Networks, *Phys. Rev. Lett.* **121**, 208301 (2018).
- [18] J. Hindes, P. Jacquod, and I. B. Schwartz, Network desynchronization by non-Gaussian fluctuations, *Phys. Rev. E* **100**, 052314 (2019).
- [19] M. Tyloo, T. Coletta, and P. Jacquod, Robustness of Synchrony in Complex Networks and Generalized Kirchhoff Indices, *Phys. Rev. Lett.* **120**, 084101 (2018).
- [20] M. Fazlyab, F. Dörfler, and V. M. Preciado, Optimal network design for synchronization of coupled oscillators, *Automatica* **84**, 181 (2017).
- [21] T. Tanaka and T. Aoyagi, Optimal weighted networks of phase oscillators for synchronization, *Phys. Rev. E* **78**, 046210 (2008).
- [22] M. Brede, Synchrony-optimized networks of non-identical Kuramoto oscillators, *Phys. Lett. A* **372**, 2618 (2008).
- [23] B. Li and K. Y. M. Wong, Optimizing synchronization stability of the Kuramoto model in complex networks and power grids, *Phys. Rev. E* **95**, 012207 (2017).
- [24] D. Kelly and G. A. Gottwald, On the topology of synchrony optimized networks of a Kuramoto-model with non-identical oscillators, *Chaos* **21**, 025110 (2011).
- [25] M. Fardad, F. Lin, and M. R. Jovanovic, Design of optimal sparse interconnection graphs for synchronization of oscillator networks, *IEEE Trans. Autom. Control* **59**, 2457 (2014).
- [26] P. S. Skardal, D. Taylor, and J. Sun, Optimal Synchronization of Complex Networks, *Phys. Rev. Lett.* **113**, 144101 (2014).
- [27] F. Dörfler and F. Bullo, Synchronization and transient stability in power networks and nonuniform kuramoto oscillators, *SIAM J. Control Optim.* **50**, 1616 (2012).
- [28] M. Alhazmi, P. Dehghanian, S. Wang, and B. Shinde, Power grid optimal topology control considering correlations of system uncertainties, *IEEE Trans. Ind. Appl.* **55**, 5594 (2019).
- [29] M. Durand, Structure of Optimal Transport Networks Subject to a Global Constraint, *Phys. Rev. Lett.* **98**, 088701 (2007).
- [30] S. Bohn and M. O. Magnasco, Structure, Scaling, and Phase Transition in the Optimal Transport Network, *Phys. Rev. Lett.* **98**, 088702 (2007).
- [31] E. Katifori, G. J. Szöllösi, and M. O. Magnasco, Damage and Fluctuations Induce Loops in Optimal Transport Networks, *Phys. Rev. Lett.* **104**, 048704 (2010).
- [32] J. W. Rocks, H. Ronellenfitch, A. J. Liu, S. R. Nagel, and E. Katifori, Limits of multifunctionality in tunable networks, *Proc. Natl. Acad. Sci. U.S.A.* **116**, 2506 (2019).
- [33] J. B. Kirkegaard and K. Sneppen, Optimal Transport Flows for Distributed Production Networks, *Phys. Rev. Lett.* **124**, 208101 (2020).
- [34] F. Kaiser, H. Ronellenfitch, and D. Witthaut, Discontinuous transition to loop formation in optimal supply networks, *Nat. Commun.* **11**, 5796 (2020).
- [35] H. Ronellenfitch, Optimal Elasticity of Biological Networks, *Phys. Rev. Lett.* **126**, 038101 (2021).
- [36] Z. G. Nicolaou, M. Sebek, I. Z. Kiss, and A. E. Motter, Coherent Dynamics Enhanced by Uncorrelated Noise, *Phys. Rev. Lett.* **125**, 094101 (2020).
- [37] J. H. Meng and H. Riecke, Synchronization by uncorrelated noise: Interacting rhythms in interconnected oscillator networks, *Sci. Rep.* **8**, 6949 (2018).
- [38] K. H. Nagai and H. Kori, Noise-induced synchronization of a large population of globally coupled nonidentical oscillators, *Phys. Rev. E* **81**, 065202(R) (2010).
- [39] H. Nakao, K. Arai, and Y. Kawamura, Noise-Induced Synchronization and Clustering in Ensembles of Uncoupled Limit-Cycle Oscillators, *Phys. Rev. Lett.* **98**, 184101 (2007).
- [40] C. Zhou, J. Kurths, I. Z. Kiss, and J. L. Hudson, Noise-Enhanced Phase Synchronization of Chaotic Oscillators, *Phys. Rev. Lett.* **89**, 014101 (2002).
- [41] H. Nakao, Phase reduction approach to synchronisation of nonlinear oscillators, *Contemp. Phys.* **57**, 188 (2016).
- [42] M. Aravind, S. Sinha, and P. Parmananda, Competitive interplay of repulsive coupling and cross-correlated noises in bistable systems, *Chaos* **31**, 061106 (2021).
- [43] R. K. Esfahani, F. Shahbazi, and K. A. Samani, Noise-induced synchronization in small world networks of phase oscillators, *Phys. Rev. E* **86**, 036204 (2012).
- [44] Y. Kuramoto, *Chemical Oscillations, Waves, and Turbulence*, Springer Series in Synergetics Vol. 19 (Springer, Berlin, Heidelberg, 1984).
- [45] J. A. Acebrón, L. L. Bonilla, C. J. Pérez Vicente, F. Ritort, and R. Spigler, The Kuramoto model: A simple paradigm for synchronization phenomena, *Rev. Mod. Phys.* **77**, 137 (2005).
- [46] F. Dörfler and F. Bullo, On the Critical Coupling for Kuramoto Oscillators, *SIAM J. Appl. Dyn. Syst.* **10**, 1070 (2011).
- [47] See Supplemental Material at <http://link.aps.org/supplemental/10.1103/PhysRevLett.128.098301> for the explicit analytical expression for the two-oscillator order parameter, an analysis of the approximations made in the main text, derivations of the two-oscillator model near a fixed point, centered dynamics, a derivation of the Lyapunov equation constraint, explanation of numerical methods, optimal noise for twisted states and periodic square grids, an analysis of the parametric dependence of the optimal noise matrices, and an analysis of second-order power grid models. The Supplemental Material includes Refs. [9,48–52].
- [48] D. A. Wiley, S. H. Strogatz, and M. Girvan, The size of the sync basin, *Chaos* **16**, 015103 (2006).
- [49] Z. Gajić and M. T. J. Qureshi, *Lyapunov Matrix Equation in System Stability and Control* (Dover Publications, Mineola, NY, 2008), p. 272.
- [50] C. Rackauckas and Q. Nie, DifferentialEquations.jl—a performant and feature-rich ecosystem for solving differential equations in Julia, *J. Open Res. Software* **5**, 15 (2017).
- [51] M. Udell, K. Mohan, D. Zeng, J. Hong, S. Diamond, and S. Boyd, Convex optimization in Julia, in *2014 First Workshop for High Performance Technical Computing in Dynamic Languages* (IEEE, New Orleans, 2014), pp. 18–28.
- [52] M. Garstka, M. Cannon, and P. Goulart, COSMO: A conic operator splitting method for large convex problems, *J. Optim. Theory Appl.* **190**, 779 (2021).
- [53] M. Schröder, M. Timme, and D. Witthaut, A universal order parameter for synchrony in networks of limit cycle oscillators, *Chaos* **27**, 073119 (2017).

- [54] L. Vandenberghe and S. Boyd, Semidefinite programming, *SIAM Rev.* **38**, 49 (1996).
- [55] University of Washington, Power systems test case archive, <https://labs.ece.uw.edu/pstca/>.
- [56] G. V. Osipov, J. Kurths, and C. Zhou, *Synchronization in Oscillatory Networks* (Springer-Verlag, Berlin Heidelberg, 2007), p. 373.
- [57] M. Tyloo, L. Pagnier, and P. Jacquod, The key player problem in complex oscillator networks and electric power grids: Resistance centralities identify local vulnerabilities, *Sci. Adv.* **5**, eaaw8359 (2019).
- [58] D. Manik, M. Rohden, H. Ronellenfitsch, X. Zhang, S. Hallerberg, D. Witthaut, and M. Timme, Network susceptibilities: Theory and applications, *Phys. Rev. E* **95**, 012319 (2017).
- [59] L. Zhu and J. Lin, Learning spatiotemporal correlations for missing noisy PMU data correction in smart grid, *IEEE Internet of Things J.* **8**, 7589 (2021).
- [60] P. E. Bett and H. E. Thornton, The climatological relationships between wind and solar energy supply in Britain, *Renewable Energy* **87**, 96 (2016).
- [61] K. van der Wiel, H. C. Bloomfield, R. W. Lee, L. P. Stoop, R. Blackport, J. A. Screen, and F. M. Selten, The influence of weather regimes on European renewable energy production and demand, *Environ. Res. Lett.* **14**, 094010 (2019).